Vol. 28 / No. 3 / Pages 265–380 *July 1996*

JOURNAL OF

THE AMERICAN SOCIETY FOR QUALITY CONTROL

QUALITY TECHNOLOGY

A Quarterly Journal of Methods Applications and Related Topics

Adaptive Control Limits for Bivariate Process Monitoring

PAVEL GRABOV

Advanced Logistics Developments Ltd., Rishon Lezion 75106, Israel

DOV INGMAN

Technion—Israel Institute of Technology, Haifa 32000, Israel

Variables control charts implement process state testing by separately assessing the measures of central tendency and spread. This work, based on the ideas of bivariate process control, analyzes whether the standard charting method could be considered as optimal and presents an alternative mode of process evaluation—biparameter description in terms of the joint distribution of sample averages and standard deviations. Thus it becomes possible to benefit from the advantages of this approach and at the same time to overcome its main shortcoming, namely lack of diagnostic ability. The proposed single $\bar{X}$ chart with adaptive control limits provides a reliable tool for recognizing process state and indicating the parameter responsible for an out-of-control state. Additionally, the proposed method does not require a constant sample size during data collection.

Introduction

ANALYSIS of the statistical behavior of a process implies a decision concerning its stability—whether the observed changes are caused by inherent variability (random fluctuations) or by so-called assignable causes (changes due to equipment deterioration, incoming material quality, employees' mistakes, etc.).

Control charts, suggested and developed by Shewhart (1981) more than 60 years ago, provide a useful and simple method (see, e.g., Porter and Caulcutt (1992)) for dealing with such problems. All control charts have a common structure. A plot of the results of repeated sampling is made on a vertical scale against the number of samples plotted horizontally. The chart centerline represents the long-term average of the process statistic or its standard value. The upper and lower control limits (UCL and LCL, respectively) represent the boundaries of typical statistic variation. Points falling outside the control limits call for adjustment. In order to detect departures from expected process behavior within the limits (so-called nonrandom patterns on the chart), different run tests for pattern recognition are used (see Nelson (1985)).

Two kinds of errors may occur when using control charts: overadjustment (personnel reacting to process variations that are merely the result of common causes) and underadjustment (an appreciable process change due to an assignable cause is not detected). These errors are caused by the uncertainty of inferences based on sampling statistics, and their magnitude depends on the decision-making method.

In the first section of the work, the standard procedure of hypothesis testing is compared with the control chart technique consisting in separate testing of hypotheses about the measures of the process central tendency and spread. It is shown that the technique is equivalent to construction of a rectangular control region whose boundary points have no mutual property; therefore, in analogy with multivariate control "both the Type I and Type II errors for a sample point correctly plotting in control are not equal to their advertised levels for the individual control charts" (Montgomery (1991)).

Dr. Grabov is Manager of the Department of Research and Training.

Dr. Ingman is a Senior Lecturer in the Department of Quality Assurance and Reliability.

In fact, the control chart method for variables represents the particular case of bivariate process control (BPC) for which the independent variables are represented by the process mean and the measure of its variability. Use of separate univariate ('uniparameter' in our case) charts for bivariate control can be misleading, so in BPC it is customary to construct an elliptical control region (dictated by the joint bivariate distribution) for the controlled variables. If a sample point plots outside the region, visual inspection may reveal which parameter is responsible for this condition.

The main disadvantage associated with the control ellipse is that on-line process surveillance is practically impossible. This shortcoming is avoided by reduction of the problem rank. In conventional BPC the one-dimensional χ^2 statistic, depending on jointly controlled quality characteristics, is computed and charted on a Hotelling's T^2 control chart (see Alt and Smith (1988)). This chart cannot distinguish between the different assignable causes of process disturbance (variation of either the first or the second variable); therefore it can only be used in conjunction with the standard Shewhart charts, which serve as auxiliary cause-recognizing charts for cases where the basic T^2 chart indicates an out-of-control state.

Reduction of the problem rank for univariate cases by plotting a statistic depending on both process mean and variance has been considered by some authors. For example, Reynolds and Glosh (1981) proposed plotting a statistic representing the squared standardized deviations of the observations from the target value. This statistic represents the current standardized counterpart of the Taguchi loss function. Monitoring the value of this function is also discussed by Derman and Ross (1994). Obviously, these charts are not intended for evaluation of process stability but its uniformity, which can be characterized by a quality loss occurring when the process deviates from its desired value and generates nonuniform products. Incidentally, these charts are incapable of distinguishing a shift in the mean from an increase in variance.

The optimal shape of the control region for the case of simultaneously controlled process mean and variability is determined in the second section. The region boundary is characterized by the same value of probability density function (pdf) of the joint sampling distribution for averages and standard deviations. It is shown that the region represents the unbiased most powerful test. The control region boundary corresponds to the critical value of the proposed one-dimensional B statistic, which depends on the sample mean and standard deviation.

The third section is devoted to development of the new charting technique based on the relationship between the sample statistics for the points bounding the control region. The chronological record of the introduced statistic (B chart) can be used for the process state testing. Compared with Shewhart charts, the B chart is characterized by reduced probability of Type II error, but cannot distinguish between the different assignable causes of an out-of-control state (in analogy with the above-mentioned charts for process uniformity evaluation).

The proposed alternative charting technique is based on correction of the $\overline{X}$ chart control limits in accordance with the shape of the true control region. The charting procedure implies continuous revision of the limits depending on the sample standard deviation. The suggested $\overline{X}$ chart with adaptive control limits characterizes the process as a whole. It contains the information about the behavior of both the central tendency ($\overline{X}$ plot) and spread (control limits). The chart combines the advantages of the standard variables charts and the BPC approach. It reduces the adjustment errors (versus the Shewhart charts), reflects the process dynamics (in contrast with the control ellipse), and retains the cause recognition ability (in contrast with Hotelling's T^2 control chart).

The last section of the work presents a case study with comparative analysis of the standard and proposed charts.

Backgound on Control Charts and Hypothesis Testing

The main goal in process state testing can be formulated as follows: "Do the results of sampling indicate that the process pdf remains the same?" Although both modern statistical theory and information theory provide many tools for solving this problem (Information Divergence, Mahalonobis Generalized Distance, etc., see, e.g., Duran and Odell (1974)), the same control charts have been used in industry for years because of their simplicity.

The charting techniques represent a continuous procedure of hypothesis testing (see, e.g., Meredith (1990), Mittag and Rinne (1993)), although many would disagree with this statement. Indeed, there are at least two significant differences between the

techniques and hypothesis testing. First, rejection of a null hypothesis in statistical process control (SPC) must be supported by a follow-up investigation to identify assignable causes, whereas the common procedure of hypothesis testing allows rejection on the basis of comparison of the test statistic with the test critical value only. Secondly, a null hypothesis in SPC can be rejected not only for salient points on a control chart but also due to nonrandom behavior of the obtained data, whereas hypothesis testing does not imply any analysis of data patterns.

Nevertheless, many SPC specialists agree that "a Shewhart control chart ... is equivalent to applying a sequence of hypothesis tests" (Chengular, Arnold, and Reynolds (1989)). The centerline represents the hypothesized mean value of the process parameter; the control limits represent the critical values of the two-sided test for the null hypothesis acceptance region, and each point represents a test value for the given sample. The alternatives in using control charts can be stated (see Diamond (1989)) as

- General Null Hypothesis (H_0): No essential difference exists between the properties of interest (given by pdf) of the two populations; versus
- General Alternative Hypothesis (H_1): A significant difference does exist between the properties of interest (given by pdf) of the two populations.

The variables control chart procedures used for comparison of populations implies two separate consecutive steps where the general null hypothesis is split into two simple null hypotheses concerning population means and variances

- First Simple Null Hypothesis (H_0): $\sigma^2 = \sigma_0^2$ versus H_1: $\sigma^2 \neq \sigma_0^2$; and
- Second Simple Null Hypothesis (H_0): $\mu = \mu_0$ versus H_1: $\mu \neq \mu_0$,

where μ_0 and σ_0 are characterized by the chart centerlines, and μ and σ are estimated by the sample statistics.

The decision-making method is the same for both the first and second steps: if the points fall outside the corresponding control limits, the null hypothesis is rejected. Rejection of at least one of the simple null hypotheses leads to rejection of the general null hypothesis. Thus, a positive decision as to whether a sampling point belongs to the universe is based on the logical *and* of the simple null hypothesis

$$\sigma^2 = \sigma_0^2 \quad \text{and} \quad \mu = \mu_0. \tag{1}$$

To determine whether the process mean is at the standard value, the control chart for averages ($\overline{X}$) is most widely used, while charts based on either the sample range R or the sample standard deviation S are used to monitor process variability. In this work, we will concentrate on the combination of $\overline{X}$–S charts, although the proposed approach is valid for the $\overline{X}$–R combination as well. Note, that according to Shewhart (1981), the S chart is preferable to the R chart for monitoring variation due to two main reasons: the standard deviation is more efficient and less dependent on the form of the parent distribution. However, in later works it was shown that the range can be successfully used for process variability charting "when its undesirable statistical characteristics are combined with its ease of application" (Nelson (1994)).

Use of separate $\overline{X}$ and S charts is equivalent to plotting $(\overline{X}, S)$ on the single graph formed by superimposing the $\overline{X}$ chart over the S chart, as shown in Figure 1. The control limits for each chart plotted on their corresponding axes form a rectangle (referred to as the *Shewhart Rectangle*) representing the control region for this $\overline{X}$–S graph. For all points falling within the Rectangle, condition (1) is met, so the general null hypothesis cannot be rejected.

Elliptical Control Region

In the present work, we suppose that the boundary of the true control region should represent a locus of points with a given mutual property. For example, in the T^2 chart the control region is bounded by an ellipse of equal χ^2-statistic values corresponding to the chart's UCL. It can be shown (see Lemma 1 and its proof in Appendix A) that for the case of no a priori information concerning possible process drift from its stable state, the most powerful test for a given significance level corresponds to a control region bounded by the locus of iso-pdf points.

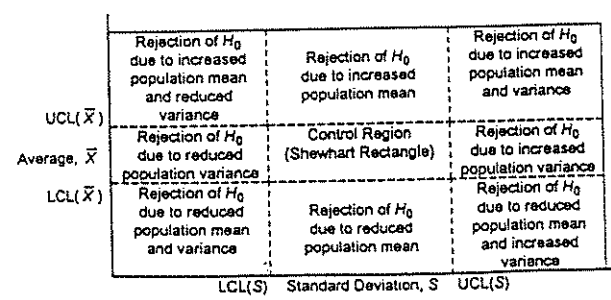

FIGURE 1. Graphical Description of the Variables Control Chart Decision-Making Method.

Taking into account the mutual orthogonality of the sample averages and standard deviations, the pdf of the joint $\bar{X}$–S distribution can be written

$$p(\bar{X}, S) = p(\bar{X})p(S)$$

where, on the assumption that samples of size n are drawn from a normal universe with parameters μ and σ, $p(\bar{X})$ and $p(S)$ denote the pdf of the sampling distribution of averages and standard deviations (see Fisher (1973)), and

$$p(\bar{X}) = \frac{1}{\sigma}\sqrt{\frac{n}{2\pi}}\exp\left[-\frac{n(\bar{X}-\mu)^2}{2\sigma^2}\right]$$

$$p(S) = \frac{2}{\sigma\Gamma\left(\frac{n-1}{2}\right)}\sqrt{\left(\frac{n-1}{2}\right)^{n-1}}\left(\frac{2}{\sigma}\right)^{n-2} \times \exp\left[-\left(\frac{n-1}{2}\right)\left(\frac{2}{\sigma}\right)^2\right].$$

The joint $\bar{X}$–S distribution corresponds to a surface in three-dimensional space (see Figure 2*a*), whose horizontal sections represent control regions (whose area depends on the given significance level α) bounded by contours of constant pdf (see Figure 2*b*). For a small sample size, $n \leq 5$, the contours have an oval shape due to the positively skewed S distribution; for $n > 5$ the contours become more elliptical. At the top of the joint distribution the control region generates into a point with coordinates $\bar{X}_{\text{mode}} = \mu$ and $S_{\text{mode}} = \sigma\sqrt{(n-2)/(n-1)}$. Introducing the standardized variables $\bar{Z} = (\bar{X}-\mu)/\sigma$ and $S^* = (S/\sigma)\sqrt{(n-1)/(n-2)}$, the pdf of the joint sampling distribution can be written

$$p(\bar{Z}, S^*) = W(n) \times \exp\left\{-\frac{n\bar{Z}^2 + (n-2)[(S^*)^2 - 2\ell\text{n}(S^*) - 1]}{2}\right\} \quad (2)$$

where

$$W(n) = \frac{1}{\Gamma\left(\frac{n-1}{2}\right)}\sqrt{\frac{n(n-2)^{n-1}}{\pi 2^{n-2}\exp(n-2)}}.$$

Obviously, the iso-pdf contour bounding the control region corresponds to the same value of the exponent power in braces, which can be designated as the B statistic

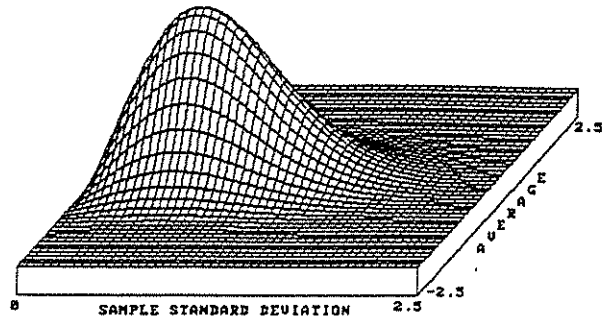

(a)

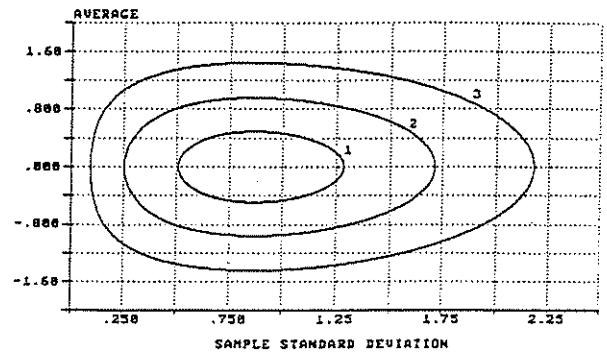

(b)

FIGURE 2. (a) The Joint $\bar{X}$–S Sampling Distribution for $n = 5$, and (b) its Contours at (1) $\alpha = 1 - (0.6826)^2 = 0.54406$, (2) $\alpha = 1 - (0.9546)^2 = 0.09974$, and (3) $\alpha = 1 - (0.9973)^2 = 0.0054$.

$$B = 0.5\{n\bar{Z}^2 + (n-2)[(S^*)^2 - 2\ell\text{n}(S^*) - 1]\}. \quad (3)$$

It can be shown that the distribution of the B statistic can be approximated by the exponential distribution with zero minimal value and unity expectation and variance (see Appendix B)

$$p(B) = \exp(-B)$$
$$B_{\min} = 0$$
$$E(B) = 1$$
$$\text{Var}(B) = 1.$$

The probability of finding a sample point $(\bar{X}, S)$ inside any iso-pdf contour is given by the B statistic and

$$\int_0^{B_{\text{crit}}} p(B)dB = 1 - \alpha. \quad (4)$$

From (3) and (4) it follows that the critical B value

is universal for any sample size and depends only on the accepted α

$$B_{\text{crit}} = -\ell n(\alpha). \tag{5}$$

Obviously, the α value could be selected more or less arbitrarily, but since it is customary to use $\alpha = 0.0027$ for the standard control charts, one can get for the joint distribution that $\alpha = 1-(1-0.0027)^2 = 0.0054$. Thus, according to (5) one can get $B_{\text{crit}} = 5.22$.

The suggested B statistic closely resembles the test developed by Neyman and Pearson (1928) to test whether a sample was drawn from a normal distribution with specified parameters. Using the adopted designations, the Neyman-Pearson statistic can be written as

$$K = 0.43429\left[\bar{Z}^2 + \frac{n-2}{n}(S^*)^2 - 2\,\ell n(S^*) - \ell n\left(\frac{n-2}{n}\right)\right].$$

The critical values for the K statistic depend on sample size and given significance level (see Nelson (1994)). Comparison of the B and K statistics shows their significant difference for small n values and almost complete coincidence for large sample size. For example, if $\mu = 0$ and $\sigma = 1$, then the control regions for $n = 5$ and $\alpha = 0.01$ can be presented using these statistics as follows:

- the B statistic:

$$\bar{X}^2 + 0.8S^2 - 1.22\,\ell n(S) \le 2.615$$

- the Neyman-Pearson statistic:

$$\bar{X}^2 + 0.8S^2 - 2\,\ell n(S) \le 3.054.$$

The control regions for $n = 50$ and the same significance level are given by

- the B statistic:

$$\bar{X}^2 + 0.98S^2 - 1.92\,\ell n(S) \le 1.164$$

- the Neyman-Pearson statistic:

$$\bar{X}^2 + 0.98S^2 - 2\,\ell n(S) \le 1.167.$$

In order to illustrate the difference between the control regions given by the different approaches, a process with normal random variation $N(0,1)$ was generated. The results of sampling (set of 1800 samples, $n = 5$) are shown in Figure 3. The ovals corresponding to the critical values of the proposed test and the Neyman-Pearson test (referred to as the B and Neyman-Pearson ovals, respectively) were computed according to $\alpha = 0.0054$. The Shewhart Rectangle was set up using the corresponding control chart factors. Figure 3 shows the significant difference between three regions—the area of the B oval is approximately 9% less than that of the Rectangle and 24% less than that of the Neyman-Pearson oval. One can see that the B oval suits best the shape of the scatter diagram, and both the empty Rectangle corners and the empty annulus bounded by the right-hand parts of ovals only increase the probability of underadjustment.

Obviously, all comparisons of the control region areas are completely meaningful only if the out-of-control distribution is uniform. The assumption about uniformity results from the absence of a priori information concerning possible process variations from its stable 'in-control' state. Therefore, one can assume that any point corresponding to the given assignable cause can appear in the sample space with the same probability (see Appendix A). Incidentally, the Shewhart Rectangle is set up implicitly from the same assumption (the two-sided alternative hypotheses with identical significance level value for the process mean and variance).

For small sample size, both the B oval and the Shewhart Rectangle have significantly more power than the Neyman-Pearson test. Since sample sizes

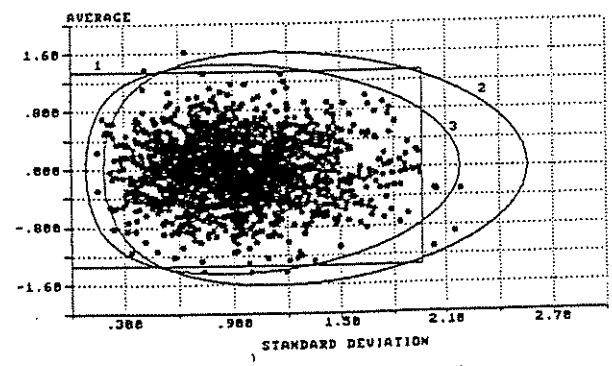

FIGURE 3. $\bar{X}$–S Graph presenting the Results of Monte Carlo Simulation for the Shewhart Rectangle (1), the Neyman-Pearson Oval (2), and the B Oval (3). * is the Sampling Data.

of four through six are quite common in industry for establishing control charts, the Neyman-Pearson statistic is inapplicable for charting purposes. For large n the power of the proposed and Neyman-Pearson tests are almost the same and exceed the power of the Shewhart technique of consecutive testing. Almost complete coincidence of the B and the Neyman-Pearson ovals for large sample size is illustrated by Figure 4.

To demonstrate the advantage of the suggested control region over the Shewhart Rectangle for small n, let us suppose that the generated process evolves along the pdf gradient line through the right-hand upper Rectangle top ($\bar{Z}$= 1.342, S^* = 2.268). The power function of the B oval against the Rectangle (for simultaneous changes in both process parameters) is shown in Figure 5 where the β value was calculated as the relative number of generated points remaining within the control region for a given shift of the process parameters. The steeper curve of the oval indicates that its power is significantly higher. Obviously, the power curve looks different for other gradients and there are cases where the traditional approach is more powerful, but as a whole a control region bounded by the locus of iso-pdf points, represents a most powerful test (see Lemma 1 in Appendix A).

Improved Charting Technique

B Chart

The chronological record of the β statistic (B chart) can be used for process state testing. B_{crit} represents the decision-making limit value, UCL.

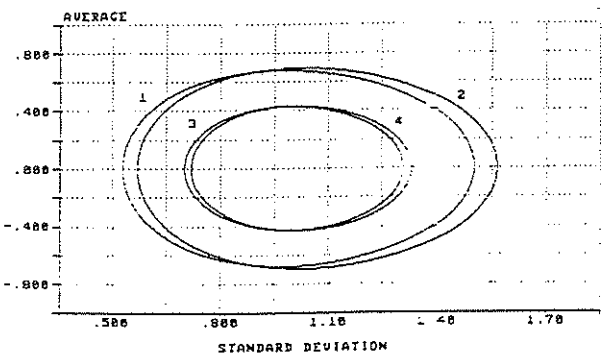

FIGURE 4. Control Ovals Corresponding to α = 0.01 and Different Sample Sizes. The B Ovals are n = 20 (1) and n = 50 (3). The Neyman-Pearson Ovals are n = 20 (2) and n = 50 (4).

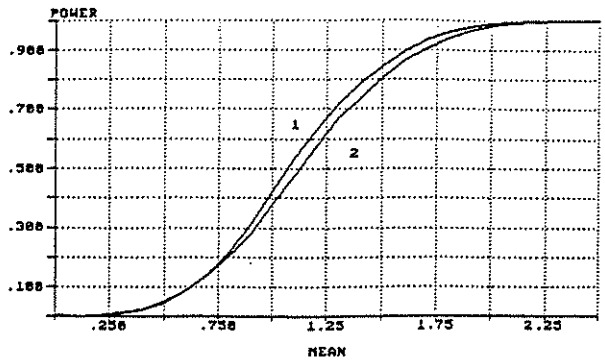

FIGURE 5. Power Function of the B Oval (1) versus the Rectangle (2).

We consider that the process is in an "in-control" state for any point satisfying the inequality $B(\bar{X}_i, S_i) \le B_{\text{crit}}$, and that it is in an "out-of-control" state if $B(\bar{X}_i, S_i) > B_{\text{crit}}$. Unlike the Shewhart charts intended for separate testing of two simple null hypotheses concerning population parameters, the B chart represents the technique for the general null hypothesis testing. Incidentally, it is shown in the work of Neyman and Pearson (1928) that separately testing the two hypotheses about process central tendency and spread is not equivalent to the technique based on "setting up the contours of equi-probable doublets $(\bar{X}, S)$" which is intended to test "whether a given sample ... has been drawn from a specified population." The one-dimensional B statistic, being an analog of the χ^2 statistic used in the conventional BPC, is characterized by the same advantage and drawback—the reduced underadjustment error is combined with the inability to distinguish between different assignable causes of process disturbance (shift in mean or increase in variance).

$\bar{X}$ Chart with Adaptive Control Limits

Rejection of the rectangular control region inevitably leads to rejection of the concept of constant control limits on process control charts. Obviously, the elliptical shape of the constructed optimal control region dictates an alternative charting technique based on adaptive control limits. The latter can be defined either by the critical values for $\bar{X}_i$ as a function of S_i or by critical values for S_i as a function of $\bar{X}_i$. Since testing of both simple null hypotheses implies setting critical values based on the measure of process spread, the dependence of the $\bar{X}$ chart limits on the sample standard deviation is the basis for the suggested technique. Taking into account that $\bar{X}_i$

and S_i for the boundary contour are related by (3) and that for pairs $(\overline{X}_i, S_i)$ falling within the control region $B_i \le B_{\text{crit}}$ substitution of (5) on the left-hand side of (3) yields the equations for the $\overline{X}$ chart limits as a function of S_i, then

$$\left\{\frac{\text{UCL}_i}{\text{LCL}_i}\right\} = \mu \pm \sigma\sqrt{|K|}\,\text{sign}(K_i) \qquad (6)$$

where UCL_i and LCL_i represent the control limit values for the i^{th} sample and

$$K_i = \frac{(n-2)[1 + 2\,\ell\text{n}(S_i^*)^2 - (S_i^*)] - 2\,\ell\text{n}(\alpha)}{n}.$$

There are three possibilities for K_i:

1. K_i is positive for any sample standard deviation between the left and right vertices of the boundary contour. Vertex values are given by the roots of the equation

$$(S^*)^2 - 2\,\ell\text{n}(S^*) = 1 - \frac{1\,\ell\text{n}(\alpha)}{n-2}.$$

2. $K_i = 0$ when the sample standard deviation is equal to the vertex values. For this case the control limits on the $\overline{X}$ chart touch each other and the central line.
3. K_i is negative for the sample standard deviation leftwards from the left vertex or rightwards from the right one.

For the 'No Standard Given' case, the corresponding sample estimates of the population parameters are used in (6) instead of σ and μ. (At the same time, the control region becomes somewhat blurred and the method sensitivity is impaired, but quantitative analysis of this case is beyond the scope of the paper.)

The above expressions imply continuous revision of the control limits on the $\overline{X}$ chart in accordance with variation of the S value, irrespective of whether S_i has exceeded the allowable limits; whereas the conventional procedure implies revision only on the full set of samples and only subject to presence of salient points on the charts. In terms of hypothesis testing, the proposed procedure requires determination of the critical values for each test, in contrast to the constant critical values on the standard $\overline{X}$ chart. The proposed chart partly resembles the charts for variable subgroup size, where due to the variable sample size, control limits must be calculated for each sample (see, e.g., Burr (1976)).

The dynamics of the $\overline{X}$ chart with adaptive control limits can be used for detecting process variability. This can be illustrated by analysis of the influence of S value variation on the behavior of the limits. There are several basic patterns on the S chart that "can occur within any given process" (Garrity (1993))

A. a jump, or tremendous shift between two consecutive points;
B. a run, or a series of consecutive points that fall on one side of the centerline;
C. a trend, or a series of consecutive points continuing to rise or fall in one direction;
D. a cycle, or a series of points displaying a similar or repeated pattern over an equal interval of time; and
E. hugging, where the points remain close to the centerline.

All these patterns and the equivalent responses of the control limits are shown in Figures 6*a* and 6*b*, respectively (the limits on the S_i chart correspond to the leftmost and rightmost points of the boundary oval for $n = 5$). One can see that the limits synchronously follow the S-value fluctuations. As the sample standard deviations concentrate in the vicinity of S_{mode}, the $\overline{X}$ chart control limits become wider. The closer the S value to the control limits on the S chart, the tighter the $\overline{X}$ chart control limits. Overlap of the limits indicates the S value exceeds its control limits (as a rule, the UCL on the S chart).

It should be emphasized that the proposed $\overline{X}$ chart with adaptive control limits contains information concerning both the central tendency and spread variations. The sensitivities of this chart and B chart to the process drift are absolutely identical, and neither requires a constant sample size during data collection. The difference between the charts is that the

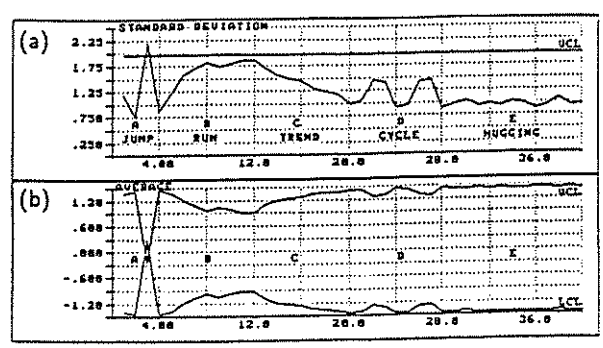

FIGURE 6. (a) Patterns on the S Chart, and (b) Control Limits on the $\overline{X}$ Chart as a Function of Sample Standard Deviation Value.

former not only provides a reliable basis for judging whether the process is in statistical control, but for an out-of-control state also indicates the parameter responsible for it.

An application example of the proposed approach is given below.

Case Study

The viscosity of the first 25 samples of size 6 were measured during the start-up phase in development of a new chemical process. These samples were used to establish the $\overline{X}$ and S charts (Figures 7*a* and 7*b*, respectively). The calculated sample statistics yielded the estimates of the universe parameters of $\overline{\overline{X}} = 37.98$ and $\overline{S} = 0.303$. Analysis of the standard $\overline{X}$–S charts shows that there are no points outside the control limits on the S chart, though four points, (6, 12, 14, and 21) are out of control on the $\overline{X}$ chart. The same data were used to construct the B chart and an $\overline{X}$ chart with adaptive limits (Figures 7*c* and 7*d*, respectively). Samples were obtained at hourly intervals over a period of three days. During this period, all technological parameters were carefully recorded. The results of charting were compared

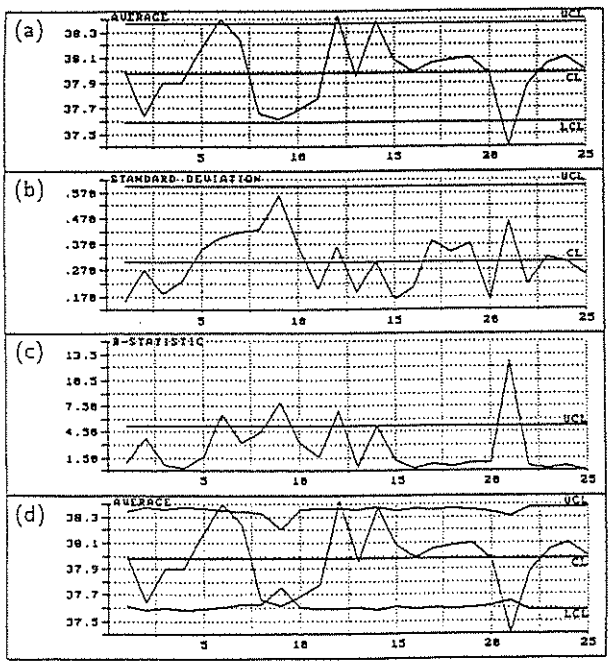

FIGURE 7. Case Study Charts for (a) Averages, (b) Standard Deviations, (c) B Statistics, and (d) $\overline{X}$ Chart with Adaptive Control Limits.

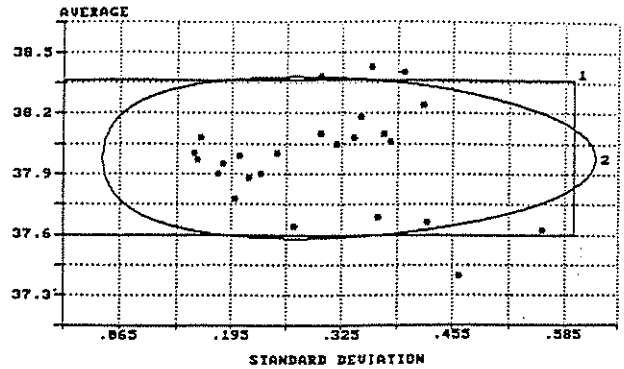

FIGURE 8. Case Study Graph for the Shewhart Rectangle (1) and the B Oval (2). * is the Sampling Data.

with the parallel technological records in order to be certain of identifying the assignable causes of all salient points on the charts.

The standard and proposed charts lead to the same conclusion at points 6, 12, and 21 and to different conclusions at points 9 and 14. Obviously, the difference is caused by the S values for these points. Point 9 lies near the LCL on the standard $\overline{X}$ chart and near the UCL on the S chart. Hence, it falls outside the control limit on both the B chart and the $\overline{X}$ chart with adaptive limits. By contrast, point 14, characterized by standard deviation near the S mode value, does not exceed the UCL on these charts.

Comparative analysis of the records and charts provided evidence (infringement of the operating regulations) for points 6, 9, 12, and 21, however no assignable cause has been discovered for point 14. Thus, the decisions based on analysis of the proposed charts are characterized by better reliability.

The B oval and Shewhart Rectangle for the case are shown in Figure 8. Visual inspection of the graph leads to the same conclusions—points 6, 12, and 21 fall outside the oval and the Rectangle; point 9 falls in the Rectangle corner and outside the oval (underadjustment); and point 14 falls inside the oval but outside the Rectangle (overadjustment).

Conclusions

The following points can be observed.

1. Process state testing by means of the standard variables control charts is equivalent to construction of a rectangular control region. It was shown that the region cannot be considered optimal.

2. The suggested optimal control region has an elliptical (oval) shape and was demonstrated to be the most powerful test (proceeding from the assumption concerning a uniform out-of-control distribution—see Appendix A). The region boundary represents the locus of points having the same pdf value of the joint sampling distribution for averages and standard deviations. The chronological record of the one-dimensional B statistic corresponding to the control region boundary can be used for process state testing.
3. The equation obtained for the boundary of the control region is used to construct an $\overline{X}$ chart with adaptive control limits. The charting procedure implies continuous revision of the limits depending on the sample standard deviation value. The proposed single chart can be used for process state testing instead of the pair of Shewhart charts for variables. It combines reliable decision making, characteristic of the BPC method, with recognition ability, typical of the standard variables charts. It also does not require a constant sample size during collection of the data.

The suggested charting technique also allows significantly increased efficiency of pattern recognition while monitoring the process. The solution of this problem using the proposed charts will be shown in further detailed research work in progress by the authors.

Appendix A

Let us introduce the two-dimensional finite sample space E with an area A in which a sample is described by a point $Y(\overline{X}, S)$. A process in this space is characterized by out-of-control and in-control states. We assume that the out-of-control subspace is identical to the E space and contains the in-control subspace. A quality control system generates sample points in the E space with different conditional probability densities

- $p(Y|H_0)$ – pdf of the sampling distribution in the in-control subspace under the condition that H_0 (general null hypothesis) is true; and
- $p(Y|H_1)$ – pdf of the sampling distribution in the out-of-control subspace under the condition that H_1 (general alternative hypothesis) is true.

In most cases $p(Y|H_0)$ is known, while on the contrary there is no a priori information concerning possible process variations from its stable in-control state (we do not consider here the rather rare situation of forecast instability described by Abraham and Kartha (1979)).

We suppose, therefore, that any point $(\overline{X}_i, S_i)$ caused by any assignable cause can appear in the out-of-control subspace with the same probability. Thus $p(Y|H_1)$ can be described by a uniform distribution (see Barnard (1959)), characterized by maximal entropy. So $p(Y|H_1)$ is given by

$$p(Y|H_1) = \frac{1}{A}$$

where A denotes a constant value depending on the E-space limits.

The control region C in E space at significance level α can be defined through the probability $1-\alpha$ of a point Y being observed within C, under the condition that H_0 (general null hypothesis) is true, that is,

$$\Pr(Y \in C|H_0) = \int\int p(Y|H_0)d\overline{X}\ dS = 1-\alpha. \tag{A1}$$

The critical region C_{crit} in E space can be defined as a totality of points not belonging to the control region C. Then at the same significance level

$$\Pr(Y \in C_{\text{crit}}|H_0) = \int\int p(Y|H_0)d\overline{X}\ dS = \alpha. \tag{A2}$$

Obviously, one can construct an infinite number of control regions with different power and the corresponding critical ones, satisfying (A1) and (A2).

Lemma 1. *A control region bounded by the locus of iso-pdf points, represents a most powerful test and has the minimal area.*

Proof. Let us introduce a control region C^* in E space, whose boundary represents the locus of points having the same pdf value p_0 (depending on the significance level). Then for the corresponding critical region C^*_{crit} in E space

$$p(Y|H_0) = \begin{cases} \le p_0, & \text{for each } Y \in C^*_{\text{crit}} \\ \ge p_0, & \text{for each } Y \notin C^*_{\text{crit}} \end{cases}. \tag{A3}$$

Dividing (A3) by the constant value $p(Y|H_1)$, we get

$$\frac{p(Y|H_0)}{p(Y|H_1)} = \begin{cases} \le Ap_0, & \text{for each } Y \in C^*_{\text{crit}} \\ \ge Ap_0, & \text{for each } Y \notin C^*_{\text{crit}} \end{cases}.$$

This is nothing less than the requirement of Neyman-Pearson theorem for the most powerful test (see, e.g., Brandt (1976)). Obviously, the test is unbiased due to its definition given by (A1).

For any other control region C, which may partly overlap with C^*, in accordance with (A2)

$$\int\int p(Y|H_0)d\bar{X}\ dS = \int\int p(Y|H_0)d\bar{X}\ dS.$$

Using the notation of Figure 9 and taking into account that F is contained in both C^* and C, we can write

$$\bar{p}^*(D+G) = \bar{p}(H+1). \qquad \text{(A4)}$$

where $\bar{p}^*$ and $\bar{p}$ are the average probability density for C^* and C, respectively. Since both $D \in C^*$ and $G \in C^*$, and both $H \notin C^*$ and $I \notin C^*$, the pdf for each point in H or I is less than the pdf for each point belonging to D or G. Moreover, it follows from (A3) that the minimal pdf in D and G is greater than or equal to the maximal pdf in H and I. Thus, it is obvious that $\bar{p}^* > \bar{p}$ and from (A4) we have that $D+G < H+I$—the control region C^* has the minimal area.

Appendix B

Let us consider the annulus bounded by two concentric elliptical contours corresponding to two values of the B statistic: B (smaller contour) and $B+dB$ (larger contour). The probability of a point Y being observed within the annulus can be written

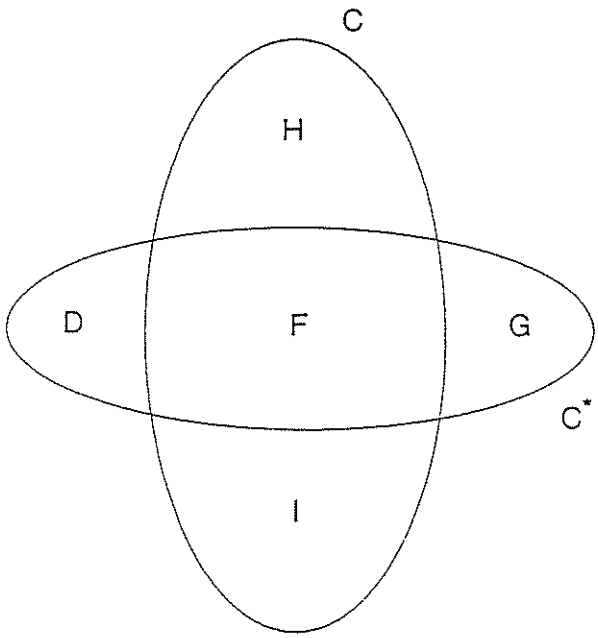

FIGURE 9. Comparison of the Areas in the Control Regions C^* and C.

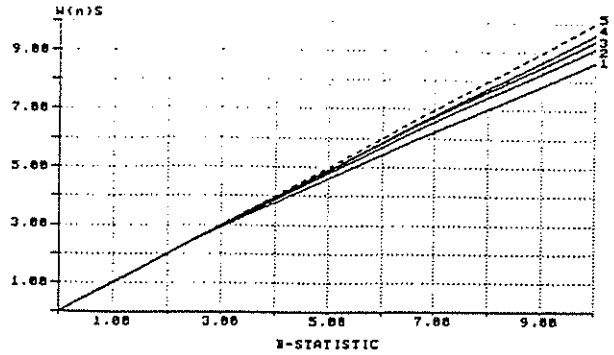

FIGURE 10. Dependencies $W(n)S$ versus B obtained by Numerical Integration.

by means of a product of iso-pdf on the smaller contour $p(\bar{Z}, S^*)$ and the annulus area dS or using the pdf of the B statistic distribution $p(B)$

$$\Pr(Y \in dS) = p(\bar{Z}, S^*)dS = p(B)dB. \qquad \text{(B1)}$$

Substituting (2) and (3) in (B1) yields

$$p(B) = W(n)\frac{dS}{dB}\exp(-B).$$

Since $S = 0$ when $B = 0$ (the peak of the joint sampling distribution), one obtains $p(B) = \exp(-B)$ if

$$W(n)S = B. \qquad \text{(B2)}$$

The dependencies $W(n)S$ versus B obtained by numerical integration with different n are shown in Figure 10. These dependencies can be written as

$$W(n)S = B - mB^p$$

where for

$n = 3$: $m = 0.02342$, $p = 1.77099$
$n = 5$: $m = 0.00630$, $p = 2.15049$
$n = 7$: $m = 0.00324$, $p = 2.27133$
$n = 10$: $m = 0.00189$, $p = 2.32515$

All these dependencies are very close to (B2), especially for $n \geq 5$ and $B \leq B_{crit} = 5.22$ (critical value for $\alpha = 0.0054$), hence the distribution of the B statistic can be approximated by the exponent with the sufficient accuracy. Accurate numerical pdf calculation for the B statistics yields for

$n = 3$: $B_{crit} = 5.08$
$n = 5$: $B_{crit} = 5.12$
$n = 7$: $B_{crit} = 5.15$
$n = 10$: $B_{crit} = 5.18$

Acknowledgments

This work was accomplished while the first author was a Senior Lecturer in the Department of Quality Assurance and Reliability at Technion—Israel Institute of Technology. His research was partially supported by the Israel Ministry of Absorption.

We thank Dr. Zigmund Bluvband, President of Advanced Logistics Developments Ltd., whose comments helped to improve this work.

References

ABRAHAM, B. and KARTHA, C. P. (1979). "Forecast Stability and Control Charts". *ASQC 33rd Annual Technical Conference Transactions*. American Society for Quality Control, Milwaukee, WI, pp. 675–680.

ALT, F. B. and SMITH, N. D. (1988). "Multivariate Process Control" in *Handbook of Statistics 7* edited by P. R. Krishnaiah and C. R. Rao. North-Holland, Amsterdam, pp. 333–351.

BARNARD, B. A. (1959). "Control Charts and Stochastic Processes" (with discussion). *Journal of the Royal Statistical Society* B 21, pp. 239–271.

BRANDT, S. (1976). *Statistical and Computation Methods in Data Analysis*. North-Holland, Amsterdam.

BURR, I. W. (1976). *Statistical Quality Control Methods*. Marcel Dekker, New York, NY.

CHENGULAR, I. N.; ARNOLD, J. C.; and REYNOLDS, M. R., JR. (1989). "Variable Sampling Intervals for Multiparameter Shewhart Charts". *Communications in Statistics – Theory and Methods* 18, pp. 1769–1792.

DERMAN, C. and ROSS, S. (1994). *Elements of Statistical Quality Control*. MacMillan College Publishing, New York, NY.

DIAMOND, W. J. (1989). *Practical Experiment Designs for Engineers and Scientists*. Van Nostrand Reinhold, New York, NY.

DURAN, B. S. and ODELL, P. L. (1974). *Cluster Analysis*. Springer-Verlag, Berlin.

FISHER, R. A. (1973). *Statistical Methods and Scientific Inference*. Hafner Press, New York, NY.

GARRITY, S. M. (1993). *Basic Quality Improvement*. Prentice Hall International Editions, Englewood Cliffs. NJ.

MEREDITH, J. P. W. (1990). *Statistical Methods in Engineering and Quality Assurance*. John Wiley & Sons, New York, NY.

MITTAG, H. J. and RINNE, H. (1993). *Statistical Methods of Quality Assurance*. Chapman and Hall, London.

MONTGOMERY, D. C. (1991). *Introduction to Statistical Quality Control*, 2nd ed. John Wiley & Sons, New York, NY.

NELSON, L. S. (1985). "Interpreting Shewhart $\bar{X}$ Control Charts". *Journal of Quality Technology* 17, pp. 163–165.

NELSON, L. S. (1994). "Did a Sample Come from a Specified Distribution?". *Journal of Quality Technology* 26, pp. 144–145.

NEYMAN, J. and PEARSON, E. S. (1928). "On the Use and Interpretation of Certain Test Criteria for Purposes of Statistical Inference". *Biometrica* 20A, pp. 175–240.

PORTER, L. J. and CAULCUTT, R. (1992). "Control Chart Design. A Review of Standard Practice". *Quality and Reliability Engineering International* 8, pp. 113–122.

REYNOLDS, M. R., JR. and GLOSH, B. K. (1981). "Designing Control Charts for Means and Variances". *ASQC Quality Congress Transactions*. American Society for Quality Control, Milwaukee, WI, pp. 400–407.

SHEWHART, W. A. (1981). *Economic Control of Quality of Manufactured Products*. Van Nostrand, New York, NY (1931). Reprint: American Society for Quality Control, Milwaukee, WI.

Key Words: *Adaptive Control Scheme, Control Limits, Statistical Process Control, Variables Control Charts.*